Inorganic Chemistry

Article

pubs.acs.org/IC

Donor-Free Phosphenium–Metal(0)–Halides with Unsymmetrically Bridging Phosphenium Ligands

Daniela Förster,[§] Jan Nickolaus,[§] Martin Nieger,[†] Zoltán Benkő,[‡,⊥] Andreas W. Ehlers,[∥] and Dietrich Gudat*[,§]

[§]Institut für Anorganische Chemie, University of Stuttgart, Pfaffenwaldring 55, 70550 Stuttgart, Germany

[†]Laboratory of Inorganic Chemistry, Department of Chemistry, University of Helsinki, P.O Box 55 (A.I. Virtasen aukio 1), 00014 Helsinki, Finland

[‡]Department of Inorganic and Analytical Chemistry, Budapest University of Technology and Economics, Szent Gellért tér 4, 1111 Budapest, Hungary

[∥]Division of Organic Chemistry, VU University Amsterdam, De Boelelaan 1083, 1081 HV Amsterdam, The Netherlands

Supporting Information

ABSTRACT: Reactions of $(cod)MCl_2$ (cod = 1,5 cyclooctadiene, M = Pd, Pt) with *N*-heterocyclic secondary phosphines or diphosphines produced complexes $[(NHP)MCl]_2$ (NHP = *N*-heterocyclic phosphenium). The Pd complex was also accessible from a chlorophosphine precursor and $Pd_2(dba)_3$. Single-crystal X-ray diffraction studies established the presence of dinuclear complexes that contain μ-bridging NHP ligands in an unsymmetrical binding mode and display a surprising change in metal coordination geometry from distorted trigonal (M = Pd) to T-shaped (M = Pt). DFT calculations on model compounds reproduced these structural features for the Pt complex but predicted an unusual C_{2v}-symmetric molecular structure with two different metal coordination environments for the Pd species. The deviation between this structure and the actual centrosymmetric geometry is accounted for by the prediction of a flat energy hypersurface, which permits large distortions in the orientation of the NHP ligands at very low energetic cost. The DFT results and spectroscopic studies suggest that the title compounds should be described as phosphenium–metal(0)–halides rather than conventional phosphido complexes of divalent metal cations and indicate that the NHP ligands receive net charge donation from the metals but retain a distinct cationic character. The unsymmetric NHP binding mode is associated with an unequal distribution of σ-donor/π-acceptor contributions in the two M–P bonds. Preliminary studies indicate that reactions of the Pd complex with phosphine donors provide a viable source of ligand-stabilized, zerovalent metal atoms and metal(0)–halide fragments.

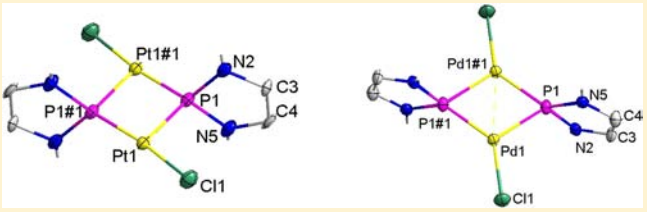

INTRODUCTION

Diaminophosphenium ions $[(R_2N)_2P]^+$ are Lewis ambiphiles that act as versatile π-acceptor ligands toward transition metals.[1−3] They resemble in this respect archetypes like CO and NO^+ yet have the advantage that their electronic and steric properties are easily tunable.[4] Computational studies suggest description of the metal–ligand bonding in phosphenium complexes with electron poor metal fragments as superposition of a dominating dative M → L π-bond and a weaker dative L → M σ-bond.[2,3] This bonding situation is qualitatively similar to that in metal carbonyls and nitrosyls or Fischer-type carbene complexes,[4−6] and the M–P bonds exhibit thus pronounced double bond character. In rare cases, phosphenium ions were also found to interact, like CO or NO^+, with two metals as μ-bridging ligands.[7,8] Although the electronic structure of such complexes has not been studied in detail, it seems reasonable to assume a partition of L → M and M → L interactions between the cationic ligand and both metal centers.

In complexes with electron-rich metals, phosphenium ions can alternatively act as essentially pure electrophiles[9] ("Z-type ligands"[10]). The L → M contribution may here be considered to be insignificant, and the interaction becomes essentially a dative M → P bond.[11] It has recently been pointed out that the variable electron demand (and the associated structural changes) of metal-bound phosphenium ions allows us to establish an analogy to the "noninnocent" behavior of nitrosyls.[12]

A unique example of electron-rich metal fragments are halide complexes of zerovalent metal atoms of the type $[L_nM^{(0)}X]^-$ (L = neutral ligand), which lack the strong electrostatic stabilization by $M^{(n+)}\cdots X^-$ Coulomb interactions. Despite their elusive nature, such species may be important reaction intermediates; for example, Amatore and Jutand suggested that anionic complexes $[Pd(PR_3)_2X]^-$ (PR_3 = tertiary phosphine, X = halide) are active participants in the widely applied Pd-catalyzed C–C bond forming reactions.[13−16] The successful stabilization of metal(0)halides by phosphenium ligands has

Received: April 9, 2013
Published: June 18, 2013

 © 2013 American Chemical Society dx.doi.org/10.1021/ic400886b | *Inorg. Chem.* 2013, 52, 7699−7708

been realized in readily isolable complexes **1** and **2** (Scheme 1),[17,18] and a similar description might also be invoked for **3**

Scheme 1[a]

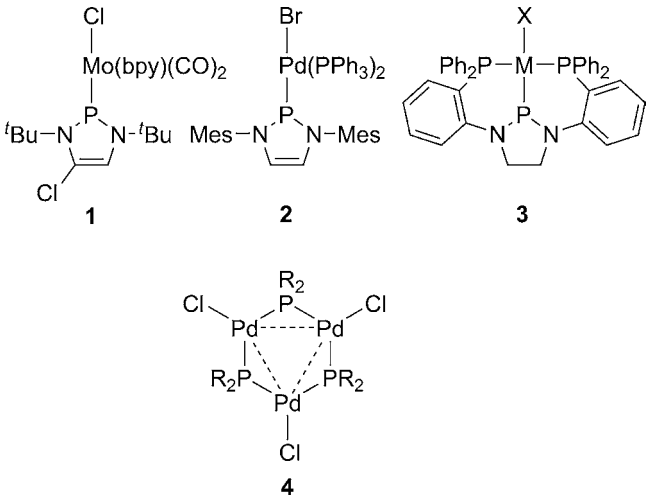

[a] **1**, bpy = 2,2′-bipyridine; **3**, M = Pd, Pt, X = Cl, Br, I; **4**, R = N^iPr_2, NCy_2.

and the trimeric complexes **4**, which had originally described as Pt(II)-phosphido complex[12] or *triangulo*-clusters with bridging phosphido ligands,[19] respectively. The phosphenium metal(0)-halides draw their stability, in simple terms, from the fact that the back-donation to the phosphenium cation and additional π-acceptor ligands decreases the electron density at the metal atom, which in turn allows for a favorable interaction with the strongly electron donating halide anion.[15,18]

In this Article, we report on dimeric complexes $[(NHP)MCl]_2$ (NHP = *N*-heterocyclic phosphenium; M = Pd, Pt), which consist, in a similar manner as **4**, of an array of metal atoms supported by μ_2-PR_2 units and terminal halides. Computational and spectroscopic studies were carried out to probe whether these products must be addressed as phosphido-bridged complexes composed of anionic R_2P-ligands and metal dications or as "donor-free" phosphenium–metal(0)–halides where the cationic ligand stabilizes an elusive metal(0)–halide fragment in the absence of ancillary donor ligands. Finally, we will present preliminary chemical reactivity studies that reveal that the dimers serve as a viable source of mononuclear metal(0) complexes.

EXPERIMENTAL SECTION

All manipulations were carried out under an atmosphere of dry argon using standard vacuum line techniques. Solvents were dried by standard procedures. NMR spectra were recorded on Bruker Avance 400 (^{1}H, 400.1 MHz; ^{13}C, 100.5 MHz; ^{31}P, 161.9 MHz; ^{195}Pt, 86.7 MHz) and Avance 250 (^{1}H, 250.1 MHz; ^{13}C, 62.8 MHz; ^{31}P, 101.2 MHz) NMR spectrometers at 303 K; chemical shifts are referenced to external TMS (^{1}H, ^{13}C), 85% H_3PO_4 (Ξ = 40.480 747 MHz, ^{31}P), or 1.2 M Na_2PtCl_6 (Ξ = 21.496 784 MHz, ^{195}Pt). Coupling constants are given as absolute values. (+)-ESI mass spectra were recorded in MeOH solution on a Bruker Daltonics MicroTOF Q instrument. Elemental analyses were determined on a Perkin-Elmer 24000CHN/O analyzer. Melting points were determined in sealed capillaries with a Büchi B-545 melting point apparatus. UV–vis spectra were recorded on a Varian Cary 50 spectrometer.

All computational studies except the calculations of NMR properties were performed with the Gaussian09[20] suite of programs. Fragment analysis of molecular orbitals and charge decomposition analyses were carried out with the program AOMIX,[21,22] and MOLDEN[23] was used for visualization. The NBO analysis was performed with the NBO 5.0 program.[24] Basis sets with electrostatic potentials (ECP) on the inner shells (cc-pVDZ(-PP), cc-pVTZ(-PP), aug-cc-pVTZ(-PP), def2-TZVP, def2-TZVPD, def2-TZVPPD) were obtained from the basis set exchange home page.[25,26] The topological analysis of the electron density was performed using different functionals (B3LYP, BP86), valence double- and triple-ζ ANO-RCC basis on the Pd/Pt atoms, and cc-pVDZ and cc-pVTZ basis set on all the other atoms. The contraction scheme applied for double-ζ all electron basis function is 6s 5p 3d 1f for Pd and 7s 6p 4d 2f 1g for Pt. The contraction scheme for triple-ζ all electron basis function is 7s 6p 4d 2f 1g for Pd and 8s 7p 5d 3f 2g for Pt. In order to take relativistic effects into consideration, Douglas–Kroll–Hess second-order (DKH2) scalar relativistic calculations[27−29] have been performed. The calculation of NMR properties was carried out using density functional theory (DFT) as implemented in the Amsterdam Density Functional (2009.01)[30] code in which an all-electron, triple-ζ, double-polarization TZ2P Slater basis was used including functions up to 5p and 4f for Pd and 6p and 5f for Pt. Relativistic two-component zero-order regular approximation (ZORA)[31−34] calculations including spin–orbit coupling[35−38] have been performed with the local density approximation (LDA) in the Vosko–Wilk–Nusair parametrization[39] with nonlocal corrections for exchange (Becke88)[40] and correlation (Perdew86)[41] included in a self-consistent manner. Isotropic absolute magnetic shieldings for the phosphorus nuclei in **6″** and **7″** were calculated using both "experimental" geometries (based on the crystallographic coordinates of **6** and **7** with hydrogen atom positions being readjusted using experimental bond and torsional angles and C–H distances of 1.09 Å) and optimized (at the BP86/cc-pVTZ-(PP) level) and converted to the common chemical shift scale using the reference data by Jameson[42] ($\delta(^{31}P) = 328 - \sigma(^{31}P)$).

Synthesis of Complex 6. *From **5** and (cod)PdCl$_2$.* Diphosphine **5**[43] (200 mg, 0.25 mmol) and 1 equiv of (cod)$PdCl_2$ (70 mg, 0.25 mmol) were dissolved in anhydrous THF (5 mL) and stirred for 15 min at room temperature. A dark green microcrystalline precipitate formed, which was filtered off, washed two times with diethyl ether, and dried under reduced pressure. The crude product was purified by recrystallization from CH_2Cl_2 at −20 °C. Yield 46%, mp >250 °C.

*From **9** and (cod)PdCl$_2$.* Secondary phosphine **9**[44] (200 mg, 0.49 mmol) and 1 equiv of (cod)$PdCl_2$ (140 mg, 0.49 mmol) were dissolved in anhydrous THF (5 mL) and stirred for 15 min at room temperature. The formed dark green, microcrystalline precipitate was filtered off, washed two times with diethyl ether, and dried under reduced pressure. Yield 43%.

*From **9** and (cod)PdCl$_2$ in the Presence of NEt$_3$.* Secondary phosphine **9** (15 mg, 37 μmol), 1 equiv of (cod)$PdCl_2$ (10 mg, 37 μmol), and 1 equiv of NEt_3 were dissolved in anhydrous d_8-THF (0.7 mL). The solution was irradiated in an ultrasonic bath for approximately 2 min. Quantitative formation of **6** and the absence of chlorodiazaphospholene **8** as byproduct were established by ^{31}P NMR spectroscopy. No attempts toward isolation of the product were made. $^{31}P\{^1H\}$ NMR (C_6D_6): δ = 225.1 (s). ^{1}H NMR (C_6D_6): δ = 7.30 (t, 4 H, $^3J_{HH}$ = 7.7 Hz, *p*-CH), 7.03 (d, 8 H, $^3J_{HH}$ = 7.7 Hz, *m*-CH), 6.82 (pseudo-t, 4 H, $^5J_{PH}$ = 5.9 Hz, NCH), 3.03 (sept, 8 H, $^3J_{HH}$ = 6.9 Hz, $CH(CH_3)_2$), 1.04 (d, 24 H, $^3J_{HH}$ = 6.7 Hz, CH_3), 0.95 (d, 24 H, $^3J_{HH}$ = 6.7 Hz, CH_3). $^{13}C\{^1H\}$ NMR (C_6D_6): δ = 147.2 (pseudo-t, $^3J_{PC}$ = 2.0 Hz, *o*-C), 132.3 (s, *i*-C), 129.7 (s, *p*-C), 129.0 (s, NCH), 124.3 (s, *m*-C), 28.9 (s, $CH(CH_3)_2$), 25.9 (s, CH_3), 24.8 (s, CH_3). (+) ESI MS: *m*/*e* (%): 1059.35(100) $[C_{52}H_{72}N_4P_2Pd_2 - OCH_3]^+$. UV–vis ($CH_2Cl_2$): λ_{max}/nm (ε_{max}/(10^3 L mol^{-1} cm^{-1})): 600 (3.3), 515 (35.1), 410 (21.2). $C_{52}H_{72}Cl_2N_4P_2Pd_2$ (1098.85): calcd C 56.84, H 6.60, N 5.10; found C 56.24, H 6.68, N 5.06; the unsatisfactory low C value is due to the inclusion of small, nonstoichiometric amounts of solvent (CH_2Cl_2, verified by ^{1}H NMR), which could not be completely removed.

Synthesis of Complex 7. A solution of diphosphine **5** (200 mg, 0.25 mmol) and 1 equiv of (cod)$PtCl_2$ (92 mg, 0.25 mmol) in anhydrous THF (5 mL) was stirred for 30 min at room temperature. The solvent was removed in vacuum. The dark red residue was

dx.doi.org/10.1021/ic400886b | Inorg. Chem. 2013, 52, 7699–7708

extracted two times with diethyl ether and dried under reduced pressure. The crude product was purified by recrystallization from CH_2Cl_2/Et_2O (2:1) at −20 °C. Yield 41%, mp >250 °C. $^{31}P\{^1H\}$ NMR (C_6D_6): δ = 26.9 (s, $^1J_{PPt}$ = 5000 Hz). $^{195}Pt\{^1H\}$ NMR (C_6D_6, 303 K): δ = −3078 (t, $^1J_{PPt}$ = 5000 Hz). ^1H NMR (C_6D_6): δ = 7.32 (t, 4 H, $^3J_{HH}$ = 7.8 Hz, *p*-CH), 7.03 (d, 8 H, $^3J_{HH}$ = 7.8 Hz, *m*-CH), 6.03 (pseudo-t, 4 H, $^5J_{PH}$ = 3.5 Hz, NCH), 3.44 (sept, 8 H, $^3J_{HH}$ = 6.9 Hz, $CH(CH_3)_2$), 0.98 (d, 48 H, $^3J_{HH}$ = 6.8 Hz, CH_3). $^{13}C\{^1H\}$ NMR (C_6D_6): δ = 148.1 (pseudo-t, $^3J_{PC}$ = 2.0 Hz, *o*-C), 133.4 (s, *i*-C), 129.3 (s, *p*-C), 124.7 (s, *m*-CH), 122.3 (s, NCH), 29.0 (s, $CH(CH_3)_2$), 25.9 (s, CH_3), 24.8 (s, CH_3). (+) ESI MS: *m*/*e* (%): 1235.47(100) $[C_{52}H_{72}N_4P_2Pt_2 - OCH_3]^+$. UV−vis ($CH_2Cl_2$): λ_{max}/nm (ε_{max}/(10^3 L mol^{-1} cm^{-1})): 495 (2.7, sh), 425 (26.9), 375 (sh). $C_{52}H_{72}Cl_2N_4P_2Pt_2$ (1276.18): calcd C 48.94, H 5.69, N 4.39; found C 48.70, H 5.84, N 4.34.

Reaction of 6 with PPh_3. Complex **6** (100 mg, 90 μmol) and 4 equiv of PPh_3 (95 mg, 0.36 mmol) were dissolved in CH_2Cl_2 (6 mL) to give an orange solution. A ^{31}P NMR spectrum recorded after 20 min showed broad signals attributable to **13** as major reaction product besides traces of **8**, $Pd(PPh_3)_3$, and a decomposition product, which was later identified by NMR spectroscopy and single-crystal X-ray diffraction as *trans*-$(PPh_3)_2PdCl_2$ (**12**). The signals of **13** sharpened into resolved multiplets at −20 °C. The amount of **8** and **12** increased continuously when the reaction mixture was stored for longer time in order to allow crystallization, up to the point that the initial product **13** disappeared completely, and **12** remained the only product that could be isolated in pure form by crystallization. ^{31}P NMR (CH_2Cl_2, 303 K): δ = 222.7 (br; **13**), 24.7 (br; **13**). ^{31}P NMR (CH_2Cl_2, 253 K): δ = 222.1 (t, $^2J_{PP}$ = 129 Hz; **13**), 24.3 (d, $^2J_{PP}$ = 129 Hz; **13**).

Reaction of 6 with $HPPh_2$. Complex **6** (50 mg, 46 μmol) and an excess of diphenylphosphine were dissolved in CH_2Cl_2 to give a red solution. A ^{31}P NMR spectrum recorded after 15 min showed signals attributable to **14** as main reaction product besides small amounts of **8** and $Pd(HPPh_2)_x$ and excess diphenylphosphine. Storage of the reaction mixture for crystallization was accompanied by eventual decomposition of **14** to give **8** and $Pd(HPPh_2)_x$ and a few crystals of $Pd(HPPh_2)_4$, which were identified by a single-crystal X-ray diffraction study, were obtained as the only isolable product. ^{31}P NMR (CH_2Cl_2, 303 K): δ = 209.9 (br, **14**), −16.3 (br; **14**). ^{31}P NMR (CH_2Cl_2, 253 K): δ = 209.4 (q, $^2J_{PP}$ = 51 Hz; **14**), −13.6 (d, $^2J_{PP}$ = 51 H; **14**).

Crystallography. Crystal structures of **6** and **7** were determined on a Nonius Kappa-CCD diffractometer at 100(2) K (**6**) or 123(2) K (**7**) using Mo Kα radiation (λ = 0.71073 Å). Direct methods (SHELXS-97) were used for structure solution. Refinement was carried out using SHELXL-97 (full-matrix least-squares on F^2), and hydrogen atoms were refined using a riding model. A semiempirical absorption correction was applied. Details of the crystal structure determinations are listed in Table 1. Crystallographic data (excluding structure factors) have been deposited with the Cambridge Crystallographic Data Centre as supplementary publication nos. CCDC-905918 (**6**) and CCDC-905010 (**7**). Copies of the data can be obtained free of charge on application to: The Director, CCDC, 12 Union Road, GB-Cambridge CB2 1EZ (fax int. +1223/336033); E-mail: deposit@ccdc.cam-ak.uk.

RESULTS AND DISCUSSION

Treatment of *N*-heterocyclic diphosphine **5** with $(cod)MCl_2$ (cod = 1,5-cyclooctadiene; M = Pd, Pt) at ambient temperature in THF produced dimeric complexes $[(NHP)MCl]_2$ (**6**, M = Pd; **7**, M = Pt) and a stoichiometric amount of *N*-heterocyclic chlorophosphine **8** (Scheme 2). A mixture of palladium complex **6** and **8** was also obtained from reaction of $(cod)PdCl_2$ with secondary *N*-heterocyclic phosphine **9**. Formation of **8** as byproduct is avoided if the reaction is carried out in the presence of an acid scavenger like NEt_3, and **6** is accessible under these conditions with higher atom efficiency from equimolar amounts of **9** and $(cod)PdCl_2$ (Scheme 2). The reaction of **9** with $(cod)PtCl_2$ yielded spectroscopically

Table 1. X-ray Details for 6 and 7

	6	7
empirical formula	$C_{52}H_{72}Cl_2N_4P_2Pd_2$	$C_{52}H_{72}Cl_2N_4P_2Pt_2$
fw (g mol^{-1})	1098.78	1276.16
T (K)	100(2)	123(2)
cryst size (mm^3)	0.83 × 0.57 × 0.35	0.08 × 0.04 × 0.02
space group	$P2_1/n$ (No. 14)	$P2_1/n$ (No. 14)
a (Å)	12.7928(3)	12.916(2)
b (Å)	14.4161(4)	13.470(2)
c (Å)	14.5891(4)	14.903(2)
β (deg)	104.2790(10)	104.63(1)
V (Å^3)	2607.43(12)	2508.7(7)
Z	2	2
D_c (Mg m^{-3})	1.40	1.69
μ (mm^{-1})	0.709	5.780
F(000)	1136	1264
θ range (deg)	3.2−30.5	2.5−25.0
reflns collected	28697	23540
unique reflns	7912	4405
R_{int}	0.017	0.114
max/min transm	0.7426/0.525	0.888/0.601
data/restraints/params	7912/0/280	4405/0/280
GOF on F^2	1.05	1.04
R1 [$I > 2\sigma(I)$]	0.021	0.061
wR2 (F^2)	0.052	0.159
largest diff. peak and hole (e Å^{-3})	0.530/−0.450	2.892/−3.564

Scheme 2[a]

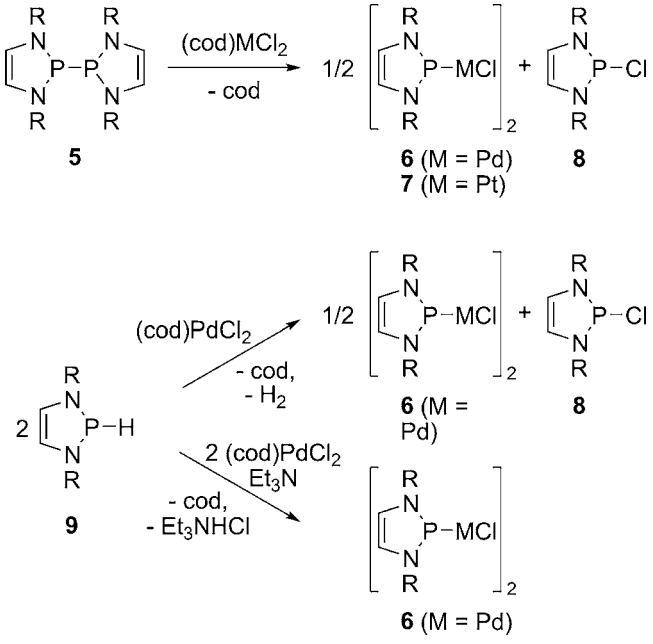

[a] R = 2,6-^{i}Pr$_2$C$_6$H$_3$.

detectable platinum hydride complexes whose isolation and full characterization is under way and will be reported elsewhere. Analysis of the ^{31}P NMR spectra of reaction mixtures revealed in all cases the absence of signals of further phosphorus-containing products and suggests thus that all reactions are quantitative. Finally, **6** is also formed, in analogy to **4**,[19] as main reaction product upon treatment of chlorophosphine **8** with an appropriate amount of $Pd_2(dba)_3$ (dba = dibenzylidene acetone).

dx.doi.org/10.1021/ic400886b | Inorg. Chem. 2013, 52, 7699−7708

Complex **6** precipitated from the solution, whereas isolation of **7** required removal of volatiles and extraction of byproducts. Both complexes were obtained as deeply colored, EPR-silent (and thus presumably diamagnetic), air-stable solids. Complex **6** is moderately soluble in CH_2Cl_2, sparingly soluble in CH_3CN, and insoluble in hydrocarbon and ether solvents (Et_2O, THF, DME); **7** showed better solubility in all solvents except Et_2O and hydrocarbons. The dimeric nature of both products was inferred from ESI-mass spectra and the pseudotriplet splittings of the ^1H NMR signals of the protons in the *N*-heterocyclic rings. In connection with the chemical equivalence of the two phosphenium moieties, these features suggest that the metal atoms are symmetrically bridged by two NHP units to form a cyclic P_2M_2 array, and each metal atom carries an extra terminal chloride (an inverse arrangement with terminal NHP and bridging chloride ligands should exhibit a very small, if not negligible, J_{PP} coupling constant and a different splitting pattern for the ^1H NMR signal of the ring protons). The ^{31}P chemical shift of 225.1 ppm for **6** is substantially lower than that for $[\{\mu\text{-}(R_2N)_2P\}PdCl]_3$[19] (**4**, $\delta^{31}P$ = 346.1 for R = *i*Pr, 351.1 for R = Cy), but the difference is of similar magnitude as in case of the free phosphenium ions (cf., $\delta^{31}P$ = 313 ppm for $(iPr_2N)_2P^{+1}$ vs 205 ppm for 1,3-bis-$C_6H_3iPr_2$-diazaphospholenium[45]). The much lower chemical shift of 26.9 ppm for **7** introduced initial doubts about the structural similarity with the Pd complex, but the presence of an analogous M_2P_2 ring was established from analysis of ^{31}P,^{195}Pt spin couplings: the ^{195}Pt NMR signal is split into a triplet ($^1J_{Pt,P}$ = 5000 Hz) indicating attachment of the metal atom to two equivalent P-donor ligands, and the ^{31}P NMR signal is accompanied by two sets of ^{195}Pt satellites due to coupling ($^1J_{Pt,P}$ = 5000 Hz) of the phosphorus atoms to one ($P_2(^{195}Pt)_1$ isotopomer, A_2X subspectrum) or two chemically equivalent metal spins ($P_2(^{195}Pt)_2$ isotopomer, A_2X_2 subspectrum), respectively.

The structural assignment was confirmed by single-crystal X-ray diffraction studies. Both complexes crystallize in the monoclinic space group $P2_1/n$ and contain isolated molecules with crystallographic C_i-symmetry. Complex **6** (Figure 1) exhibits a planar P_2Pd_2 ring in which adjacent bonds differ slightly in length (P1−Pd1 2.2738(4) vs P1−Pd1#1 2.2401(4) Å) but opposite bonds remain equal. The Pd−P−Pd angles are much more acute (71.61(1)°) than the P−Pd−P angles (108.39(1)°). The Pd−P bonds are naturally longer than those to the terminal phosphenium ligands in **2**[18] (2.117(2) Å) or $[(NHP)Pd(PPh_3)_2]OTf$[18] (Pd−P 2.1229(11) Å, NHP = 1,3-dimesityl-1,3,2-diazaphospholenium) and lie between the two distinctly different P···Pd distances in **10**[12] (Scheme 3) of 2.162(2) and 2.498(2) Å. The planar diazaphospholene rings in **6** are perpendicular to the P_2Pd_2 ring (dihedral angles 89.1° between P_2Pd_2 and PN_2C_2 planes) and mutually parallel (dihedral angle 0° between both PN_2C_2 planes). The angles between the P1−Pd1/P1−Pd1#1 bonds and the bisecting NHP ring plane are 50° and 22°, and the diazaphospholene units adopt thus a distinctly asymmetrical coordination (Figure 1b). The chlorine ligands lie in the plane of the P_2Pd_2 ring, but the Cl−Pd−P angles show likewise a marked dissymmetry (Cl1−Pd1−P1#1 134.35(2)° vs Cl1−Pd1−P1 117.27(2)°). Taking all disparities in Pd−P distances, P−Pd−Cl angles, and the alignment of diazaphospholene rings together, the observed molecular structure can be conceived to picture an early stage in the dissociation of a hypothetical dinuclear complex with ideal D_{2h} symmetry into two monomeric Cl−Pd−NHP units

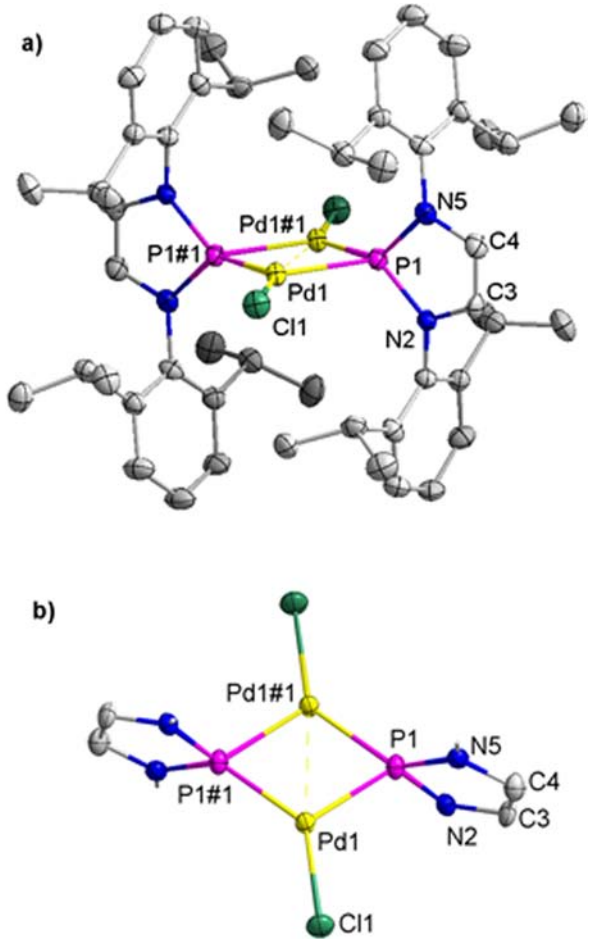

Figure 1. Representation of the molecular structure of **6** (top) and the $Pd_2P_2(NHP)_2$ core (bottom) in the crystal. H atoms were omitted for clarity; thermal ellipsoids were drawn at the 50% probability level. Selected bond lengths (Å) and angles (deg): Pd1−P1 2.2738(4), Pd1−P1#1 2.2401(4), Pd1−Cl1 2.3361(4), Pd1−Pd1#1 2.6410(2), P1−N2 1.680(1), P1−N5 1.685(1), N2−C3 1.384(2), C3−C4 1.349(2), C4−N5 1.384(2), P1#1−Pd1−P1 108.39(1), Pd1#1−P1−Pd1 71.61(1), P1−Pd1−Cl1 117.27(2), P1#1−Pd1−Cl1 134.35(2), Cl1−Pd1−Pd1#1 170.87(1), N2−P1−N5 89.55(5).

Scheme 3

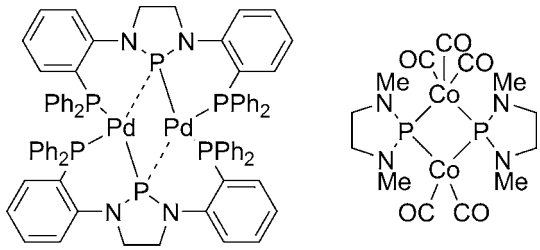

10 **11**

featuring linear dicoordinate metal and planar tricoordinate phosphorus atoms.

The coordination modes of chloride and phosphenium ligands in **6** are qualitatively similar to those in the *triangulo*-cluster **4**,[19] whose structural disorder precludes a more quantitative comparison; the different degree of aggregation in both compounds is presumably due to different steric requirements of the phosphenium moieties. The unsymmetrical

dx.doi.org/10.1021/ic400886b | *Inorg. Chem.* 2013, 52, 7699−7708

μ-bridging coordination of the aminophosphenium ligands resembles the semibridging coordination mode of carbonyls and has precedence in dipalladium and dicobalt complexes **10**[12] and **11**[7] (Scheme 3) where the geometrical distortion may be facilitated by different metal coordination environments (**11**) or the constraints imposed by the formation of chelate rings (**10**). A further interesting feature of **6** is the presence of a short metal−metal distance (2.6410(2) Å), which is only slightly larger than the distance of 2.58 Å calculated from covalent radii[46] and falls well into the range of Pd−Pd bonds in dimeric Pd(I) complexes (2.72 ± 0.1 Å[47]). The P−N, C−N, and C−C bond lengths in the PN_2C_2 rings match those of known chlorodiazaphospholenes and NHPs[45] and indicate that **1** shows, like these compounds, a certain degree of π-electron delocalization in the N-heterocyclic rings.

The molecular structure of platinum complex **7** (Figure 2) displays the same topology as **6** but exhibits some remarkable deviations in the coordination environment of the phosphorus and platinum atoms. The shape of the central ring is conserved, but the alternation of adjacent bonds (Pt1−P1 2.239(3), P1−Pt1#1 2.179(3) Å) is now even more pronounced. The bridging NHP units show a comparable tilt as in **6** (angles of the P1−Pt1 and P1−Pt1#1 vectors with the local PN_2 plane containing the atoms P1, N2, and N5 are 57° and 42°, respectively), but the difference in Cl−Pt−P bond angles is much larger than in **6** (P1−Pt1−Cl1 107.3(1)°, P1#1−Pt1−Cl1 171.7(1)°). The metal coordination geometry remains planar but is best described as T-shaped (with the nearly collinear P1#1−Pt1 and Pt1−Cl1 bonds representing the bar of the T) rather than distorted trigonal. As a consequence of this distortion, endocyclic P−Pt−P angles are much smaller (81.0(1)°) and Pt−P−Pt angles larger (99.0(1)°) than the corresponding angles in **6** (P−Pd−P 108.39(1)°, Pd−P−Pd 71.61(1)°), and the Pt···Pt distance across the ring increases to 3.360(1) Å, which rules out any direct bonding interaction. The bonds in the diazaphospholene ring of **7** are generally slightly shorter than those in **6** and closer to appropriate bond lengths in phosphenium ions.[45] In contrast to the free cations, the PN_2C_2 ring in **7** is not planar but displays a distinct envelope conformation. The Pt1−Cl1 bonds (2.268(3) Å) are slightly shorter than normal Pt−Cl distances (2.33 ± 0.04 Å[48]).

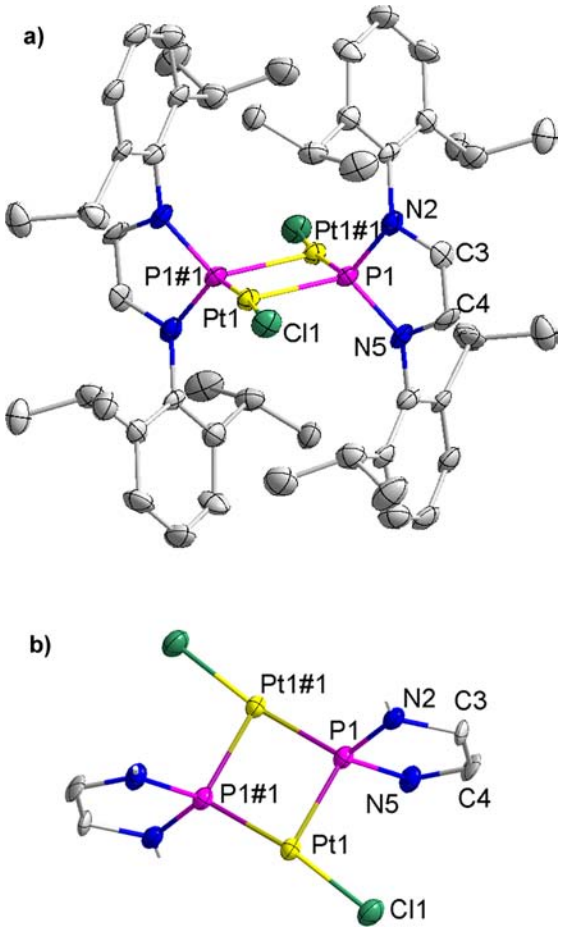

Figure 2. Representation of the molecular structure of **7** (top) and the $Pt_2P_2(NHP)_2$ core (bottom) in the crystal. H atoms were omitted for clarity; thermal ellipsoids were drawn at the 50% probability level. Selected bond lengths (Å) and angles (deg): Cl1−Pt1 2.268(3), Pt1−P1 2.239(3), Pt1−P1#1 2.179(3), Pt1−Pt1#1 3.360(1), P1−N5 1.654(10), P1−N2 1.668(11), N2−C3 1.375(15), C3−C4 1.342(17), C4−N5 1.373(16), P1#1−Pt1−P1 81.0(1), P1#1−Pt1−Cl1 171.7(1), P1−Pt1−Cl1 107.3(1), N5−P1−N2 91.2(5), Pt1#1−P1−Pt1 99.0(1).

The observed molecular structures of **6** and **7** allow for a similar ambiguity in the interpretation of metal−ligand interactions as had been discussed for other phosphenium complexes.[12] In principle, two limiting descriptions can be given: (1) the NHP units act as anionic phosphido ligands that bind as μ-bridging four-electron σ/π-donors to two metal(II) centers, and (2) the NHP units represent phosphenium cations and bind as σ-donor/π-acceptor ligands to two zerovalent metal atoms. Alternatively, complex **6** may, in view of the short intermetallic distance, also be conceived to contain two σ-bonded Pd(I) centers that bind two chlorides and two neutral diazaphospholenyl radicals (which are then antiferromagnetically coupled to give a diamagnetic product). The depiction as metal(0) complexes with formally cationic NHP ligands adheres more closely to the common perception of N-heterocyclic phosphenium ions as paramount electrophiles,[1,3] but recent reports on the noninnocence of some chelating N-heterocyclic phospheniums[12] and the proven generation of neutral diazaphospholenyl radicals[43,49] implies that the alternative descriptions may not be a priori ruled out.

In order to shed further light on the electronic structure of complexes **6** and **7**, we performed DFT calculations[20] on suitable model compounds. Anticipating that the peripheral isopropyl groups in **6** and **7** should have negligible impact on the electronic structure of the P_2M_2 core, initial computations were carried out on N-phenyl-substituted model compounds **6′** and **7′**. These studies revealed that the molecular core interacts only weakly with the substituents at nitrogen and that the computed molecular geometries and electron populations are quite similar to those of the still simpler NH-substituted species **6″** and **7″**. We therefore chose these compounds, which are much easier to handle computationally, as models for a more comprehensive electronic structure investigation.

In view of the marked structural deviation between **6** and **7**, we searched first for possible stationary points on the potential energy hypersurfaces of model complexes **6″** and **7″**. To this end, we performed energy optimizations in different restricted symmetries (C_{2v}, C_{2h}, D_{2h}) and tested several combinations of density functionals (BP86, B3LYP, M06-2X, PBE1PBE) and basis sets (cc-pVDZ(-PP), aug-cc-pVDZ(-PP), cc-pVTZ(-PP), def2-TZVP, def2-TZVPD, def2-TZVPPD) to establish an appropriate computational level. The results of these calculations are all qualitatively similar even if relative energies

dx.doi.org/10.1021/ic400886b | Inorg. Chem. 2013, 52, 7699−7708

of isomeric structures may change with the functional applied (a complete listing is given as Supporting Information), and we will only discuss the results obtained at the BP86/cc-pVTZ-(PP) level. The geometries, relative energies, and numbers of imaginary vibrational modes for stationary states of **6″** and **7″** located under different symmetry constraints (C_{2v}, C_{2h}, D_{2h}) at this level are displayed in Figure 3.

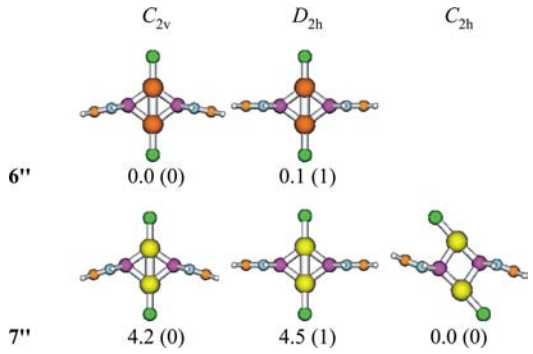

Figure 3. Geometries, relative energies (kcal mol^{-1}), and numbers of imaginary vibrational modes (in parentheses) of the isomeric structures of complexes **6″** and **7″** calculated under different symmetry constraints at the BP86/cc-pVTZ-(PP) level.

In the case of the palladium complex **6″**, the C_{2v}-structure was identified as the only local minimum. The D_{2h}-structure is a transition state at negligibly higher energy (0.1 kcal mol^{-1}), and optimization attempts in C_{2h}-symmetry (or still lower C_2- and C_i-symmetry) converged always to the D_{2h}-structure, even with small optimization steps. The computed bond distances (Table 2) agree reasonably with the experimental ones, but the overall molecular structure of **6″** differs subtly from the observed structure of **6**: the pairs of shorter and longer Pd−P bonds occupy adjacent rather than opposite edges of the P_2Pd_2 quadrangle, and the tips of the PN_2C_2 pentagons of both phosphenium ligands point to the same rather than different metal atoms.[50] The negligible energy differences between the C_{2v}- and D_{2h}-isomers as well as the energy profiles produced during the course of the geometry optimization imply that the molecular structure of **6″** tolerates large distortions in the alignment of the phosphenium ligands with hardly any energetic cost. We conclude that a reliable prediction of the molecular structure is therefore beyond the accuracy of the computational model and that the observed geometry of **6** is presumably enforced by the large steric demand of the *N*-aryl substituents or intermolecular ("crystal packing") forces.

For the platinum complex **7″**, three stationary states were found: the structures with C_{2h} and C_{2v} symmetry represent local minima, and the one with D_{2h} symmetry represents a transition state. The C_{2h}-isomer is more stable by some 4 kcal mol^{-1} than the C_{2v}-isomer, and the energy difference between the C_{2v}-isomer and the D_{2h}-transition state is also larger than in the case of **6″**. The computed molecular structure of the stable C_{2h}-isomer of **7″** is in reasonable agreement with the found structure of solid **7** (selected distances are given in Table 1 for **7″** and in Figure 2 for **7**). In addition, the low energy of the D_{2h}-transition state implies that dynamic inversion of the bridging NHP units is easily feasible and serves thus to explain the A_2X_2-type coupling patterns in ^{31}P and ^{195}Pt solution NMR spectra (which are at odds with a static C_{2h}-structure). The perceptible energy difference between the C_{2h}- and C_{2v}-isomers of **7″** suggests further that the special metal coordination geometry in **7** is not imposed by crystal packing effects. A similar supremacy of T-shaped over regular trigonal metal coordination had also been predicted for mercury halide dimers $(HgX_2)_2$ and was convincingly explained as arising from relativistic contraction (and concomitant energetic stabilization) of the mercury 6s-orbital.[51] Since this effect becomes even more important for the 6s-orbital at Pt but not for the 5s-orbital at Pd,[52] we conclude that it may also explain the deviating metal coordination geometries in **6″** and **7″**. This view is supported by the finding that the calculated natural electron configurations (see below) reveal that the contribution of the valence s-orbital of the metal atoms is much higher for Pt than for Pd.

The consideration of relativistic effects helps also in the explanation of the remarkably large difference in ^{31}P NMR chemical shifts of **6** and **7**. Relativistic two-component zero-order regular approximation (ZORA)[31−34] calculations with inclusion of spin−orbit coupling[35−38] on the model compounds **6″** and **7″** produced values of δ^{31}P (232.8 ppm for **6″** and 37.4 ppm for **7″** based on experimental geometries; cf. Table 3) that closely match the experimental data of **6** (δ^{31}P = 225.1 ppm) and **7** (δ^{31}P = 26.9 ppm), respectively. Analysis of individual contributions reveals that the stronger shielding of the ^{31}P nuclei in the Pt complex is due to two major effects, namely, a reduction in the (nonrelativistic) paramagnetic shielding contribution ($\Delta\sigma^{para}$ = 86.68 ppm) and a shift from a small negative to a large positive value of the (relativistic) spin−orbit contribution ($\Delta\sigma^{SO}$ = 106.94 ppm). Comparison of shieldings calculated with different sets of atomic coordinates (derived from the crystal structure data of **6** and **7** and the energy-optimized molecular geometries of **6″** and **7″**) indicates that the numerical values of calculated shieldings are, not unexpectedly, strongly sensitive to variations in the molecular

Table 2. Selected Bond Lengths (*d*, in Å), Wiberg Bond Indices (WBI), and Mayer Bond Indices (MBI) for 6″ (C_{2v}), 7″ (C_{2h}), and the Free Diazaphospholenium Cation ($PN_2C_2H_4^+$) at the BP86/cc-pVTZ(-PP) Level[a]

	6″ (C_{2v})	7″ (C_{2h})	$PN_2C_2H_4^+$
M−M	2.696 (0.307/0.252)	3.442 (0.146/0.148)	
M−Cl	2.317 (0.723/0.823)	2.294 (0.748/0.949)	
	2.298 (0.726/0.839)		
M−P	2.244 (0.735/0.897)	2.214 (0.821/1.250)	
	2.296 (0.654/0.847)	2.300 (0.692/0.905)	
P−N	1.723 (0.887/1.097)	1.718 (0.846/1.076)	1.695 (1.077/1.291)
N−C	1.384 (1.172/1.181)	1.393 (1.137/1.141)	1.369 (1.246/1.234)
C−C	1.361 (1.631/1.595)	1.356 (1.673/1.627)	1.374 (1.536/1.501)

[a]Entries are given in the form *d* (WBI/MBI).

dx.doi.org/10.1021/ic400886b | Inorg. Chem. 2013, 52, 7699−7708

Table 3. Computed ^{31}P NMR Chemical Shifts ($\delta(^{31}P)$) and Diamagnetic (σ^{dia}), Paramagnetic (σ^{para}), and Spin-Orbit (σ^{SO}) Contributions to the Absolute Isotropic Shielding (σ^{iso}) of 6″ and 7″[a]

	6″	7″
σ^{dia}	960.51 (959.36)	962.28 (961.14)
σ^{para}	−853.41 (−888.43)	−766.73 (−828.60)
σ^{SO}	−11.85 (−17.23)	95.09 (57.70)
σ^{iso}	95.25 (53.70)	290.64 (190.24)
$\delta(^{31}P)$	232.75 (274.30)	37.36 (137.76)

[a]Data are based on the experimental geometries of crystalline **6** and **7**; values derived from calculated geometries of 6″ and 7″ are given in parentheses.

geometries, whereas the relative magnitudes of the relativistic and nonrelativistic contributions to the total magnetic shielding variation remain relatively unaffected.

To get further insight into the bonding situation, we performed natural bonding orbital[53] (NBO) calculations on the lowest energy structures of 6″ and 7″. Analysis of bond lengths, Wiberg bond indices (WBI) and Mayer bond indices (MBI) of 6″ and 7″ (Table 1) revealed that the M−Cl and M−P bonds exhibit sizable covalent contributions, which are generally slightly higher for the Pt than the Pd complex; furthermore, the shorter M−P bonds in each species exhibit slightly larger covalent contributions than the longer ones. The P−N and N−C bonds in the NHP ligands are somewhat longer (weaker) and the C−C bonds shorter (stronger) than in the free phosphenium ion.

Even if the participation of each phosphorus atom in the formation of two M−P bonds does not a priori rule out a description of 6″ and 7″as phosphido complexes (with anionic σ-donor/π-donor ligands that bind to two M^{2+} cations), the alternative picture of phosphenium−metal(0)-species with cationic NHP ligands and metal oxidation numbers close to zero seems more appropriate for several reasons:

(i) Analysis of NPA (natural population analysis) charges (Table 4) yields negative partial charges for the metal atoms

Table 4. NPA Partial Charges (au) of the Metal Centers (M = Pd, Pt), Chlorine Atoms, and NHP Units of 6″ (C_{2v}) and 7″ (C_{2h}) at the BP86/cc-pVTZ(-PP) level

	6″ (C_{2v})	7″ (C_{2h})
M (Pd or Pt)	−0.32/−0.40	−0.35
Cl	−0.44/−0.43	−0.38
$PC_2N_2H_4$	+0.79	+0.73

and substantial positive partial charges for the diazaphospholene units in both complexes. Likewise, the calculated natural electron configurations of the metal atoms (6″ Pd1 $4d^{9.31}$ $5s^{0.51}$ $p^{0.51}$, Pd2 $4d^{9.32}$ $5s^{0.48}$ $p^{0.59}$; 7″ Pt $5d^{9.14}$ $6s^{0.85}$ $p^{0.35}$) agree better with the picture of zerovalent d^{10}-metal centers, which form dative bonds via ligand-to-metal σ-donation and metal-to-ligand π-back-donation, than with the perception of $M^{2+}(d^8)$ cations, which act predominantly as electron acceptors (the description is also supported by the Mulliken charges, see Supporting Information).

(ii) In the case of 7″, the ligand contributions dominate in the NBOs representing the "short" M−P bonds (25.1% Pt vs 74.9% P), and the metal contributions dominate in the "long" M−P bonds (60.1% Pt vs 39.9% P), suggesting that the M_2P_2 array contains two types of dative bonds of opposite polarity. The situation in 6″ is less easily interpreted since the NBO results imply a delocalized structure, which must obviously be depicted in terms of resonance between several canonical formulas. Still, the leading Lewis structure contains an array of two chloride ions, a Pd(0) atom, and a dicationic fragment $[Pd(NHP)_2]^{2+}$, which is itself composed of two phosphenium ions binding to a zerovalent metal atom, and may thus likewise be considered to support a description as phosphenium−metal(0)−halide. The unsymmetrical coordination of the NHP fragments in both 6″ and 7″ contrasts further with the symmetrical arrangement of bridging phosphides.

(iii) The decrease in P−N and N−C bond orders and concomitant increase of C−C bond orders upon complexation (see Table 2) suggest that the transfer of extra electron density to the NHP cations (as revealed by the lower partial charge for the bound ligand) raises the population of the phosphenium π_4-orbital (the LUMO of the free cation, which is PN and CN antibonding and CC bonding in character), which emphasizes the π-acceptor property of the ligand.

(iv) A charge decomposition analysis[54,55] (CDA) indicates that M_2Cl_2 → NHP electron donation is larger in 6″ (M = Pd) by 0.25 electrons and in 7″ (M = Pt) by 0.50 electrons than electron donation in the other direction. The observed figures are in line with the larger M−P bond indexes in 7″ compared with 6″ (Table 2) and further accentuate that the NHP fragments in both complexes retain substantial phosphenium (σ-donor/π-acceptor) character.

The rather short Pd1−Pd1#1 distance in **6** suggests the possibility of direct Pd···Pd bonding. Analysis of the Wiberg and Mayer bond indexes reveal that the appropriate values in 6″ are indeed larger than those in 7″, and an AIM (atoms in molecules[56,57]) analysis of the electron density of 6″ allowed us to locate, in addition to the bond critical points representing the cyclic array of M−P bonds, a further bond critical point between the palladium atoms (Figure 4). In contrast, no direct bond path between the metal atoms was found in the M_2P_2 region of 7″ (Figure 5).

Even if these topological differences seem to support the idea of direct Pd···Pd bonding in 6″, some critical issues remain: the Pd−Pd bond order (Table 2) is still far from that expected for a full bond, the position of the Pd···Pd bond critical point in 6″ is close to the adjacent ring critical points, and the electron density at this point (ρ = 0.050 au) is only marginally higher than that at the P_2Pt_2 ring critical point of 7″ (0.037 au), which represents the electron density *minimum* in this region. All features together imply that the valence charge concentration on the Pd···Pd "bond path" of 6″ is rather petty, and disfavor thus a description of the complex as containing two genuinely σ-bonded Pd(I) centers. We cannot rule out that the additional bond critical point in 6″ reflects simply the effect of trailing electron density from two metal atoms that are coerced into close positions and conclude that neither population nor topological analysis allows a clear-cut assessment of the metal−metal interaction. Two further bond critical points were identified between the C═C bonds in the NHP units and the chlorine atoms of 7″ but are in view of the still lower electron density (ρ = 0.005 au) likewise attributed to represent trailing electron density rather than a genuine bonding interaction.

In order to study the metal−ligand interaction from a different angle, we recorded UV−vis spectra of **6** and **7**. The visible region of the spectra contains three bands (λ_{max} = 600,

dx.doi.org/10.1021/ic400886b | Inorg. Chem. 2013, 52, 7699−7708

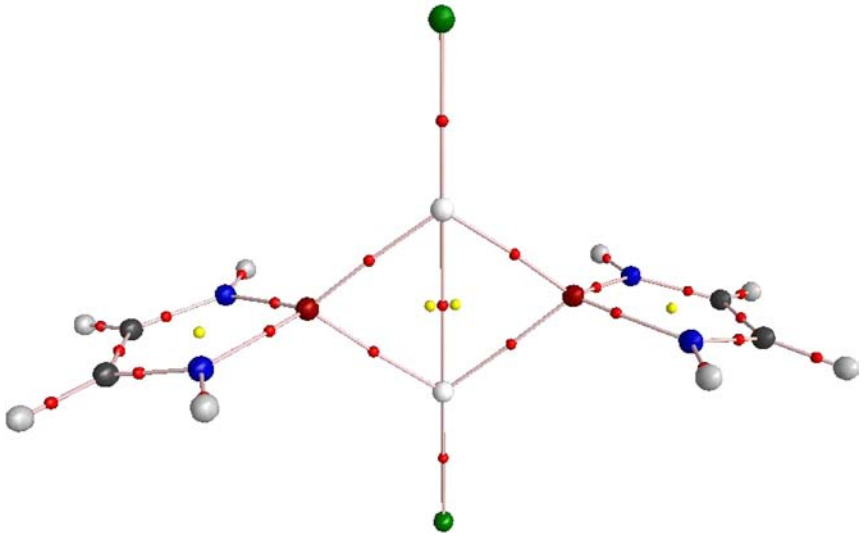

Figure 4. AIM analysis of the electron density (calculated at the BP86/cc-pVTZ (light atoms), triple-ζ-ANO-RCC(Pd)//BP86/cc-pVTZ(-PP) level) of **6″**. The lines connecting atoms represent bond paths, and the red and yellow points represent bond and ring critical points, respectively.

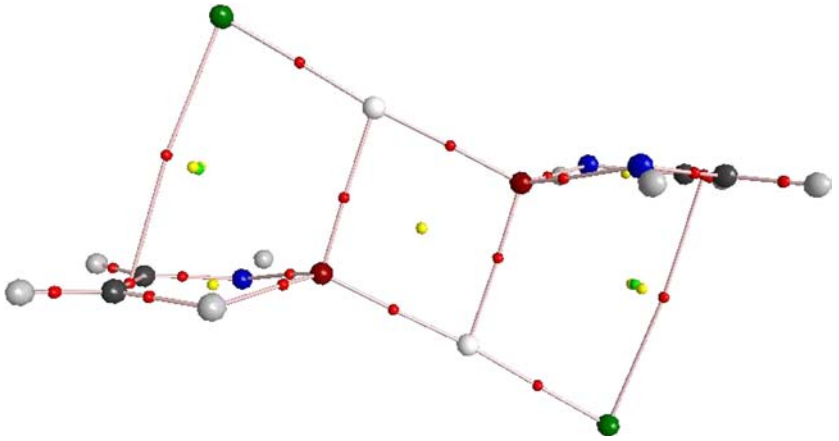

Figure 5. AIM analysis of the electron density (calculated at the BP86/cc-pVTZ(light atoms), triple-ζ-ANO-RCC(Pt)//BP86/cc-pVTZ(-PP) level) of **7″**. The lines connecting atoms represent bond paths, and the red, yellow, and green points represent bond, ring, and cage critical points, respectively.

515, and 410 nm) for **6** and two bands (λ_{max} = 495 and 425 nm) and a shoulder at shorter wavelengths for **7**. The first two absorption bands in both spectra give similar intensity patterns, but the absorption maxima of **7** are red-shifted by 90−100 nm. These features were reproduced in simulated electronic spectra of **6″** and **7″**, which had been generated from the results of TDDFT calculations (see Supporting Information; the weaker coincidence between observed and calculated transition energies for **6**/**6″** is presumably attributable to the larger deviation between computed and experimentally observed molecular structures). The TDDFT computations indicate that a single electronic transition contributes to the first and two transitions to the second spectral bands and that each transition involves a combination of several one-electron excitations. Analysis of the contributions from metal atoms, chlorides, and NHP ligands to the MOs involved in the individual one-electron excitations implies that all three electronic transitions of **6″** and the third lowest excitation of **7″** have perceptible MLCT character. The first electronic transition in **7″** is not associated with large shifts in electron population between fragments, and the second transition exhibits some LMCT character. In summary, these results can be considered as further manifestation for the π-acceptor character of the phosphenium ligands in **6** and **7**.

Finally, the view of complex **6** as phosphenium−metal(0)−halide with a formally zerovalent metal complex is supported by the outcome of preliminary reactivity studies. Reaction of **6** with 4 equiv of Ph_3P produces a darkly colored solution that contains according to a ^{31}P NMR survey a major reaction product together with minor amounts of chlorophosphine **8**, $Pd(PPh_3)_n$, and *cis*-$(Ph_3P)_2PdCl_2$ (**12**). The signals of the main product appear at −20 °C as resolved multiplets (AX_2 spin system with δ = 222.1 (P^A), 24.3 (P^X); J_{AX} = 129 Hz) and broaden at ambient temperature. The spectral parameters match those of Pd(0) bromide **2** ($\delta^{31}P$ 23.4 and 213.9[18]) and the ionic Pd(0) triflate, $[(N_2P^{Mes})(PPh_3)_2Pd]OTf$ ($\delta^{31}P$ 23.0 and 213.0, J_{PP} = 138 Hz[18]), and the product is on this basis assigned as monomeric Pd(0) halide **13** (Scheme 4). The temperature dependent line broadening had previously been observed for **2** and was explained as resulting from reversible halide dissociation and formation of a dynamic equilibrium between neutral **2** and a cation $[(N_2P^{Mes})(PPh_3)_2Pd]^+$.[18]

dx.doi.org/10.1021/ic400886b | *Inorg. Chem.* 2013, 52, 7699−7708

Scheme 4

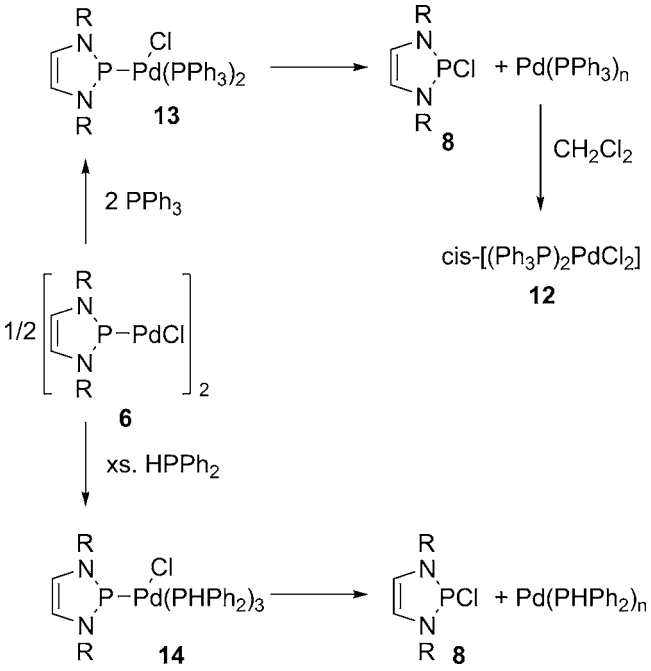

Complex **13** decomposed eventually to give **8** and **12**, which remained the only species that could be isolated in pure form. The decomposition can be envisaged to proceed via "non-reductive" elimination to form **8** and $Pd(PPh_3)_n$, which then reacts with the solvent (CH_2Cl_2) to produce **12**. This scheme allows us also to explain the formation of the byproducts observed in the initial reaction mixture. In a similar manner, **6** reacted with excess $HPPh_2$ to produce a solution containing complex **14** (^{31}P NMR, AX_3 spin system with δ = 209.4 (P^A), −13.6 (P^X); J_{AX} = 51 Hz; Scheme 4) and traces of **8** and $Pd(HPPh_2)_n$ together with unreacted phosphine. Storage of the reaction mixtures at low temperature resulted in isolation of a few crystals of $[Pd(HPPh_2)_4]$,[58] which remained the only product to be isolated.

CONCLUSION

Dinuclear complexes $[(NHP)MCl]_2$ (M = Pd (**6**), Pt (7); NHP = *N*-heterocyclic phosphenium fragment) were prepared by several routes. The products feature terminal chloride ligands and bridging NHP units and are thus structural analogues of previously reported trinuclear clusters **4**,[19] which were, mainly because of formal reasons, denoted as phosphido complexes. In contrast, evidence from computational, spectroscopic, and chemical studies suggests that **6** and **7** should be correctly addressed as genuine phosphenium−metal(0)−halides with metal oxidation numbers close to zero and ligands that receive net back-donation from the metal atoms but retain their nature as cationic phosphenium ligand. This description is in line with the recently postulated "noninnocent" behavior of amino-phosphenium ligands[12] and allows us to conclude that formal clustering of individual electronically unsaturated {ClM(NHP)} units renders the metal atoms less electron-rich than the addition of extra donor ligands. Adopting this description of phosphenium−metal(0) complexes, the reaction of $Pd_2(dba)_3$ with an *N*-heterocyclic chlorophosphine to give **6** must be considered another example of a "nonoxidative" addition[59] of a phosphenium−Lewis base adduct to a metal complex. Furthermore, the preparation of **6** and **7** from diphosphine **5** emphasizes the nature of **5** as an unusual reducing agent for metal cations and stimulates further studies to widen its application.

Several aspects deserve further consideration: (i) Compounds **6** and **7** extend the limited number of complexes with unsymmetrically μ-bridging phosphenium units. Computational studies indicate that this special binding mode, which resembles the semibridging coordination of carbonyls,[7] correlates with an uneven distribution of σ-donor and π-acceptor interactions in the P−M bonds and evokes a description of the dinuclear units as dimers of two [ClM(NHP)] monomers. This view is in accord with both the structural distortions and the easy cleavage of the dinuclear unit by donor ligands. This reactivity opens interesting possibilities to use **6** and **7** (and possibly also trinuclear species like **4**) as synthons for coordinatively and electronically unsaturated metal centers and should stimulate studies of their application as stoichiometric or catalytic reagents. (ii) The computational studies give evidence of a flat potential energy hypersurface, which allows large distortions in the alignment of the phosphenium ligands in **6** and **7** at very low energetic cost (<1 kcal mol^{-1}). Apart from providing a viable explanation for the apparently higher symmetry of the molecular structure in solution and the astonishing deviation of the computed molecular structures of model compound **6′** from that of solid **6**, a structural dichotomy between structures with like and different metal coordination environments may provide an entry point to a rich chemistry, which stimulates further studies on these and analogous complexes. (iii) In view of the fact that, regardless of all structural differences, the electronic structures of the Pd and Pt complexes **6″** and **7″** bear great similarities, the large difference in ^{31}P NMR chemical shifts cannot be considered to reflect simply the differences in charge transfer, as had been suggested,[12] and further efforts to obtain a satisfactory explanation of observed trends in magnetic shielding seem necessary.

ASSOCIATED CONTENT

Supporting Information

Experimental and simulated UV−vis spectra of **6**/**6″** and **7**/**7″**, electronic transition energies for **6″** and **7″** from TDDFT calculations at BP86/cc-pVTZ(-PP) level, Mulliken partial charges (au) of the metal centers (M = Pd, Pt), chlorine atoms, and NHP units of **6″** and **7″** at the BP86/cc-pVTZ(-PP) level, relative energies and number of imaginary frequencies for the different structures of **6″** and **7″** at different levels of theory, and total energies and coordinates of **6″** and **7″** at different levels of theory. This material is available free of charge via the Internet at http://pubs.acs.org.

AUTHOR INFORMATION

Corresponding Author

*Fax: +4971168564241. E-mail: gudat@iac.uni-stuttgart.de.

Present Address

⊥ZB: Department of Chemistry and Applied Biosciences, ETH-Zürich, Wolfgang-Pauli-Strasse 10, 8093 Zürich, Switzerland.

Notes

The authors declare no competing financial interest.

ACKNOWLEDGMENTS

We thank the Academy of Finland for a Research Fellowship and the Deutsche Forschungsgemeinschaft (DFG, Grant Gu

415/11-2) and Deutscher Akademischer Austauschdienst (DAAD) for financial support. We further thank J. Trinkner for measurement of mass spectra, Dr. W. Frey (both from Institute of Organic Chemistry, University of Stuttgart) for the collection of X-ray data sets, and Prof. László Nyulaszi (Budapest University of Technology and Economics) for helpful discussions. The bw-grid project[60] is acknowledged for supplying computational resources.

REFERENCES

(1) Cowley, H.; Kemp, R. A. *Chem. Rev. J.* **1985**, *85*, 367.
(2) Gudat, D. *Coord. Chem. Rev.* **1997**, *163*, 71.
(3) Nakazawa, H. *Adv. Organomet. Chem.* **2004**, *50*, 107.
(4) Abrams, M. B.; Scott, B. L.; Baker, R. T. *Organometallics* **2000**, *19*, 4944.
(5) Caputo, C. A.; Jennings, M. C.; Tuononen, H. M.; Jones, N. D. *Organometallics* **2009**, *28*, 990.
(6) Rosenberg, L. *Coord. Chem. Rev.* **2012**, *256*, 606.
(7) Hutchins, L. D.; Light, R. W.; Paine, R. T. *Inorg. Chem.* **1982**, *21*, 266.
(8) King, R. B.; Fu, W.-K.; Holt, E. M. *Chem. Commun.* **1984**, 1439.
(9) Hutchins, L. D.; Duesler, E. N.; Paine, R. T. *Organometallics* **1982**, *1*, 1254.
(10) Green, M. L. H. *J. Organomet. Chem.* **1995**, *200*, 127.
(11) Burck, S.; Daniels, J.; Gans-Eichler, T.; Gudat, D.; Nättinen, K.; Nieger, M. *Z. Anorg. Allg. Chem.* **2005**, *631*, 1403.
(12) Pan, B.; Xu, Z.; Bezpalko, M. W.; Foxman, B. M.; Thomas, C. M. *Inorg. Chem.* **2012**, *51*, 4170.
(13) Amatore, C.; Azzabi, M.; Jutand, A. *J. Am. Chem. Soc.* **1991**, *113*, 8375.
(14) Amatore, C.; Jutand, A.; Suarez, A. *J. Am. Chem. Soc.* **1993**, *115*, 9531.
(15) Amatore, C.; Jutand, A. *Acc. Chem. Res.* **2000**, *33*, 314.
(16) Kozuch, S.; Shaik, S.; Jutand, A.; Amatore, C. *Chem.—Eur. J.* **2004**, *10*, 3072.
(17) Gudat, D.; Haghverdi, A.; Nieger, M. *J. Organomet. Chem.* **2001**, *617*, 383.
(18) Caputo, A.; Brazeau, A. L.; Hynes, Z.; Price, J. T.; Tuononen, H. M.; Jones, N. D. *Organometallics* **2009**, *28*, 5261.
(19) Dyer, P. W.; Fawcett, J.; Hanton, M. J.; Mingos, D. M. P.; Williamson, A.-M. *Dalton Trans.* **2004**, 2400.
(20) Calculations were carried out using the Gaussian program suite: Frisch, M. J.; Trucks, G. W.; Schlegel, H. B.; Scuseria, G. E.; Robb, M. A.; Cheeseman, J. R.; Scalmani, G.; Barone, V.; Mennucci, B.; Petersson, G. A.; Nakatsuji, H.; Caricato, M.; Li, X.; Hratchian, H. P.; Izmaylov, A. F.; Bloino, J.; Zheng, G.; Sonnenberg, J. L.; Hada, M.; Ehara, M.; Toyota, K.; Fukuda, R.; Hasegawa, J.; Ishida, M.; Nakajima, T.; Honda, Y.; Kitao, O.; Nakai, H.; Vreven, T.; Montgomery, J. A., Jr.; Peralta, J. E.; Ogliaro, F.; Bearpark, M.; Heyd, J. J.; Brothers, E.; Kudin, K. N.; Staroverov, V. N.; Kobayashi, R.; Normand, J.; Raghavachari, K.; Rendell, A.; Burant, J. C.; Iyengar, S. S.; Tomasi, J.; Cossi, M.; Rega, N.; Millam, J. M.; Klene, M.; Knox, J. E.; Cross, J. B.; Bakken, V.; Adamo, C.; Jaramillo, J.; Gomperts, R.; Stratmann, R. E.; Yazyev, O.; Austin, A. J.; Cammi, R.; Pomelli, C.; Ochterski, J. W.; Martin, R. L.; Morokuma, K.; Zakrzewski, V. G.; Voth, G. A.; Salvador, P.; Dannenberg, J. J.; Dapprich, S.; Daniels, A. D.; Farkas, O.; Foresman, J. B.; Ortiz, J. V.; Cioslowski, J.; Fox, D. J. *Gaussian 09*, revision A.02; Gaussian, Inc.: Wallingford, CT, 2009.
(21) Gorelsky, S. I.; Lever, A. B. P. *J. Organomet. Chem.* **2001**, *635*, 187.
(22) Gorelsky, S. I. *AOMix: Program for Molecular Orbital Analysis*; University of Ottawa, 2012, http://www.sg-chem.net/.
(23) Schaftenaar, G.; Noordik, J. H. *J. Comput.-Aided Mol. Des.* **2000**, *14*, 123.
(24) Glendening, E. D.; Badenhoop, J. K.; Reed, A. E.; Carpenter, J. E.; Bohmann, J. A.; Morales, C. M.; Weinhold, F. *NBO 5.0*; Theoretical Chemistry Institute, University of Wisconsin, Madison, 2001.
(25) Feller, D. J. *J. Comput. Chem.* **1996**, *17*, 1571.
(26) Schuchardt, K. L.; Didier, B. T.; Elsethagen, T.; Sun, L.; Gurumoorthi, V.; Chase, J.; Li, J.; Windus, T. L. *J. Chem. Inf. Model.* **2007**, *47*, 1045. (https://bse.pnl.gov/bse/portal)
(27) Douglas, M.; Kroll, N. M. *Ann. Phys.* **1974**, *82*, 89.
(28) Hess, B. A. *Phys. Rev. A* **1985**, *32*, 756.
(29) Hess, B. A. *Phys. Rev. A* **1986**, *33*, 3742.
(30) te Velde, G.; Bickelhaupt, F. M.; Baerends, E. J.; Fonseca Guerra, C.; van Gisbergen, S. J. A.; Snijders, J. G.; Ziegler, T. *J. Comput. Chem.* **2001**, *22*, 931. ADF 2002.01: http://www.scm.com.
(31) Schreckenbach, G.; Ziegler, T. *J. Phys. Chem.* **1995**, *99*, 606.
(32) Schreckenbach, G.; Ziegler, T. *Int. J. Quantum Chem.* **1997**, *61*, 899.
(33) Wolff, S. K.; Ziegler, T. *J. Chem. Phys.* **1998**, *109*, 895.
(34) Wolff, S. K.; Ziegler, T.; van Lenthe, E.; Baerends, E. J. *J. Chem. Phys.* **1999**, *110*, 7689.
(35) Dickson, R. M.; Ziegler, T. *J. Phys. Chem.* **1996**, *100*, 5286.
(36) Khandogin, J.; Ziegler, T. *Spectrochim. Acta A* **1999**, *55*, 607.
(37) Autschbach, L.; Ziegler, T. *J. Chem. Phys.* **2000**, *113*, 936.
(38) Autschbach, L.; Ziegler, T. *J. Chem. Phys.* **2000**, *113*, 9410.
(39) Vosko, S. H.; Wilk, L.; Nusair, M. *Can. J. Phys.* **1992**, *99*, 84.
(40) Becke, A. D. *Phys. Rev. A* **1988**, *38*, 3098.
(41) Perdew, J. P. *Phys. Rev. B* **1986**, *33*, 8822.
(42) Jameson, C. J.; De Dios, A.; Jameson, A. K. *Chem. Phys. Lett.* **1990**, *167*, 574.
(43) Förster, D.; Dilger, H.; Ehret, F.; Nieger, M.; Gudat, D. *Eur. J. Inorg. Chem.* **2012**, 3989.
(44) Burck, S.; Gudat, D.; Nieger, M.; Du Mont, W.-W. *J. Am. Chem. Soc.* **2006**, *128*, 3946.
(45) Burck, S.; Gudat, D.; Nättinen, K.; Nieger, M.; Niemeyer, M.; Schmid, D. *Eur. J. Inorg. Chem.* **2007**, 5112−5119.
(46) Cordero, B.; Gómez, V.; Platero-Prats, A. E.; Revés, M.; Echeverría, J.; Cremades, E.; Barragán, F.; Alvarez, S. *Dalton Trans.* **2008**, 2832.
(47) Mean value and standard deviation of the result of a query in the CSD database for Pd−Pd distances in dinuclear palladium(I) complexes.
(48) Mean value and standard deviation of the result of a query in the CSD database for Pt−Cl distances in complexes with metal coordination numbers of 4 or less.
(49) Edge, R.; Less, R. J.; McInnes, E. J. L.; Müther, K.; Naseri, V.; Rawson, J. M.; Wright, D. S. *Chem. Commun.* **2009**, 1691.
(50) A similar molecular structure was recently established by both X-ray diffraction and computational studies on a nickel complex $[(PN_2^{Mes})NiCl]_2$ (PN_2^{Mes} = 1,3-dimesityl1,3,2-diazaphospholidinium) with analogous composition to **6** and **7**: R. T. Baker, personal communication. Hamilton, C. W.; Morris, D. E.; Blair, M. W. ; Henson, N. J.; Martin, R. L.; Cross, J. L.; Sutton, A. D.; Jantunen, K. C.; Scott B. L.; Baker, R. T. INOR 50-When is addition of X-Y to M not oxidative? Presented at the 235th American Chemical Society National Meeting, New Orleans, LA, 2008. See also ref 6.
(51) Kaupp, M.; von Schnering, H. G. *Inorg. Chem.* **1994**, *33*, 2555.
(52) Pyykkö, P. *Chem. Rev.* **1988**, *88*, 563.
(53) Reed, A. E.; Weinstock, R. B.; Weinhold, F. *J. Chem. Phys.* **1985**, *83*, 735.
(54) Dapprich, S.; Frenking, G. *J. Phys. Chem.* **1995**, *99*, 9352.
(55) Frenking, G.; Fröhlich, N. *Chem. Rev.* **2000**, *100*, 717−774.
(56) Bader, R. F. W. *Chem. Rev.* **1991**, *91*, 893.
(57) Bader, R. F. W.; Popelier, P. L. A.; Keith, T. A. *Angew. Chem.* **1994**, *106*, 647−659; *Angew. Chem., Int. Ed. Engl.* **1994**, *33*, 620−631.
(58) Leoni, P.; Marchetti, F.; Papucci, S.; Pasquali, M. *J. Organomet. Chem.* **2000**, *593*−*594*, 12.
(59) Abrams, M. B.; Hardman, N. J.; Pribisko, M. A.; Gilbert, T. M.; Martin, R. L.; Kubas, G. J.; Baker, R. T. *Angew. Chem., Int. Ed. Engl.* **2004**, *43*, 1955.
(60) bwGRiD (http://www.bw-grid.de), member of the German D-Grid initiative, funded by Federal Ministry for Education and Research and the Ministry for Science, Research and Arts Baden-Württemberg.